01,07

# Evolution of the structure of amorphous $Al_{87}Ni_8Y_5$ alloy under ultrasonic treatment

© V.V. Chirkova, N.A. Volkov, G.E. Abrosimova

Osipyan Institute of Solid State Physics RAS,
Chernogolovka, Russia

E-mail: valyffkin@issp.ac.ru

*Received November 18, 2024*
*Revised December 4, 2024*
*Accepted December 5, 2024*

The evolution of the structure of the amorphous $Al_{87}Ni_8Y_5$ alloy under ultrasonic treatment was studied using X-ray structural analysis. It was found that after ultrasonic treatment, a small amount of aluminum nanocrystals is formed. The size of the nanocrystals depends on the treatment conditions: a change in the power and duration of ultrasonic treatment leads to an increase in the average size of the nanocrystals. The reasons for the formation of nanocrystals in the amorphous phase under ultrasonic treatment are discussed in terms of free volume.

**Keywords:** metallic glasses, crystallization, nanocrystals, free volume, X-ray diffraction.

DOI: 10.61011/PSS.2025.01.60581.310

## 1. Introduction

The recent development of science and technology has been particularly in need of the development of functional materials with a unique set of performance characteristics. Obviously, the development of lightweight and particularly durable materials is a priority in the age of saving energy and natural resources. Such materials include amorphous aluminum-based alloys [1–3]. Al-TM-RE alloys are the most attractive among amorphous aluminum-based alloys, where TM is a transition metal, RE is a rare earth element, with an aluminum content of 80 to 90 at.%. These alloys exhibit extremely high strength, combined with their low specific gravity [4–6]. For example, the strength of an amorphous alloy $Al_{87}Ni_5Y_8$ is 1 GPa with a density of only 3.3 g/cm$^3$, which is approximately 2−3 times greater than the strength of traditional aluminum-based crystalline alloys [7]. It is known that the formation of nanocrystals in the amorphous phase leads to a noticeable improvement in the physical properties [8–10]. The authors of Ref. [8] have shown for the first time that the strength of an aluminum-based alloy can reach 1.6 GPa when nanocrystals are formed in the amorphous phase. It is natural to expect that the nanostructure parameters (phase composition, fraction of the crystalline phase, size of nanocrystals, and others) will play a major role in the manifestation of the unique properties of nanocrystalline alloys formed from amorphous alloys [11–13].

The heat treatment of the amorphous phase is the main method of obtaining a nanostructure. The partial crystallization of the amorphous phase in Al-TM-RE alloys in case of heating (or exposure at a constant temperature) has been studied in detail in many papers [10,14–16]. The crystallization of the amorphous phase under the impact of plastic deformation has been intensively studied in recent years [17–20]. Plastic deformation of amorphous alloys (at room temperature) is localized in shear bands [21]. Shear bands are regions with a thickness of $\sim 20$ nm where the density of the amorphous phase significantly differs from the density of the surrounding amorphous phase. It has been shown that the density in the shear bands can be 1−10% lower than the density of the amorphous phase in the surrounding matrix [22]. Such a decrease of density in the shear bands means that the content of free volume is increased in these areas [23]. The free volume is an integral characteristic of the amorphous phase [24], and its content in the amorphous phase strongly depends on the conditions for obtaining the amorphous alloy. The content of free volume in the amorphous phase decreases in case of heat treatment due to its release to the surface; the content of free volume increases in case of deformation. An increase of the free volume content in the amorphous phase was observed using various plastic deformation methods [23,25–28]. An increase of free volume means an increased distance between atoms, therefore, the content (fraction) of free volume in the sample plays a crucial role in phase transformations during heat treatment and/or deformation, and, in particular, in the formation of a nanostructure. For example, the processes of crystallization of the amorphous phase during deformation begin in the shear bands and their surroundings.

Ultrasonic treatment which is another method of treatment of the amorphous phase has been of great interest recently. The ultrasonic treatment method also leads to an increase of the free volume content in the amorphous phase [29–31]. It has been shown in some studies that the free volume content depends on the conditions of ultrasonic treatment [30,31]. It was also found that the ductility of alloys markedly increases under ultrasonic treatment, which the authors of Ref. [29] attribute to an increase (or redistribution) of the free volume. The currently available

papers are mainly devoted to the study of the effect of ultrasound on the physical properties of amorphous alloys; very little attention has been paid to studies of changes of the structure of the amorphous phase in case of such treatment. There are many studies of the effect of ultrasonic treatment on crystal formation in a liquid. For example, it was shown in Ref. [32–34] that ultrasonic treatment promotes the crystallization of the liquid phase; cavitation processes play an essential role in this process. The situation is not so clear in the case of crystallization of the amorphous phase, the literature data are quite contradictory. On the one hand, it is known that ultrasonic treatment can promote the restoration of an amorphous structure, the so-called „rejuvenation" [35]. Ultrasonic treatment can lead to crystallization of the amorphous phase according to other studies [36]. Such different results are obviously related to the peculiarities of the processes of crystallization of amorphous alloys. At least two factors can be noted. When a crystal is formed in the liquid phase (melt), the crystallization process may stop due to the release of heat of transformation; in the case of crystallization of an amorphous metal alloy, the released heat of transformation heats up the area surrounding the growing crystal, the crystallization process accelerates, and can be explosive under certain conditions. The occurrence of mechanical stresses around the growing crystal is another important factor. Since the density of the crystalline phase is higher than that of the liquid phase, the formation and growth of crystals is accompanied by an increase of stresses around the growing crystal. Unlike liquid crystallization, the process of crystallization of amorphous alloys takes place at relatively low temperatures (much lower than the melting point), under conditions of significantly slower diffusion. Since the formation of crystals in the amorphous phase in most cases follows the primary crystallization reaction by the diffusion mechanism, the redistribution of elements is much slower than at temperatures close to the formation of a melt (liquid phase). This work is devoted to the study of the effect of ultrasonic treatment on the structure of one of the representatives of light high-strength alloys of the type Al-TM-RE, namely, the amorphous alloy $Al_{87}Ni_8Y_5$.

## 2. Materials and methods

Ingot of Al-Ni-Y alloy (8 at.% Ni and 5 at.% Y) was produced by arc melting in purified argon from pure Al (> 99.99%) and Ni (> 99.9%) and compound of $Al_3Y$ (99.7%). The ingot was melted several times before melt quenching to increase the degree of uniformity. The amorphous alloy of $Al_{87}Ni_8Y_5$ was produced in the form of as a ribbon by high-speed quenching of the melt onto a rapidly rotating copper disk (cooling rate $10^6$ K/s). The ribbon thickness was 40 $\mu$m.

Samples of amorphous ribbon were subjected to ultrasonic treatment in an ultrasonic bath (power 100 W) and in an ultrasonic disperser (power 1600 W). The duration of ultrasonic treatment of the samples was 120 and 270 min. The structure of the samples before and after ultrasonic treatment was studied using Rigaku SE SmartLab X-ray diffractometer (radiation Cu $K_\alpha$, wavelength $\lambda = 1.541$ Å). Special programs were used for the processing and analysis of X-ray patterns to correct, smooth and subtract the background, as well as to separate overlapping peaks. The structure of the amorphous phase was analyzed using the Ehrenfest equation, which makes it possible to estimate the radius of the first coordination sphere $R_1$ (the shortest distance between atoms) using the experimental scattering curve [37]

$$2R_1 \sin\theta = 1.23\lambda,$$

where $\lambda$ is the wavelength of the X-ray radiation used, $\theta$ is the scattering angle.

The crystal size was determined from X-ray diffraction analysis using the Selyakov-Scherrer formula [38]

$$L = \frac{\lambda}{\Delta(2\theta) \cdot \cos\theta},$$

where $L$ is the crystal size, $\Delta(2\theta)$ is the half-width of the corresponding reflection.

## 3. Results

### 3.1. Ultrasonic bath treatment

The X-ray diffraction patterns of the samples (before, after ultrasonic treatment) were analyzed in the region of the first diffusion peak. This is attributable to the fact that the most accurate values of the structure parameters (size and proportion of crystals) can be obtained in the range with a minimum contribution of the background [39]. Figure 1 shows the X-ray diffraction patterns of the samples (the area of the first diffuse halo): *1* — the original sample that was not exposed to ultrasonic treatment, *2* — the sample that was treated in an ultrasonic bath for 120 min. A slight increase of the intensity of the diffusion peak is observed on the X-ray diffraction pattern of the sample after ultrasonic treatment. An increase of intensity when the background of the X-ray diffraction patterns coincides indicates a decrease of the half-width of the diffusion peak. This means that the peaks becomes a superposition of curves corresponding to diffusion scattering from the amorphous phase and diffraction reflection from the crystalline phase. Thus, an increase of the intensity of the diffusion peak is an evidence of the onset of the crystallization process as a result of ultrasonic treatment. The observed difference of intensity is small, but repeated measurements allow concluding that the obtained data are reproducible. It should also be noted that both X-ray patterns are not symmetrical: an additional arm is observed from the side of large angles $2\theta$. The presence of an additional arm on X-ray patterns is a sign of the separation of the initially homogeneous amorphous phase.

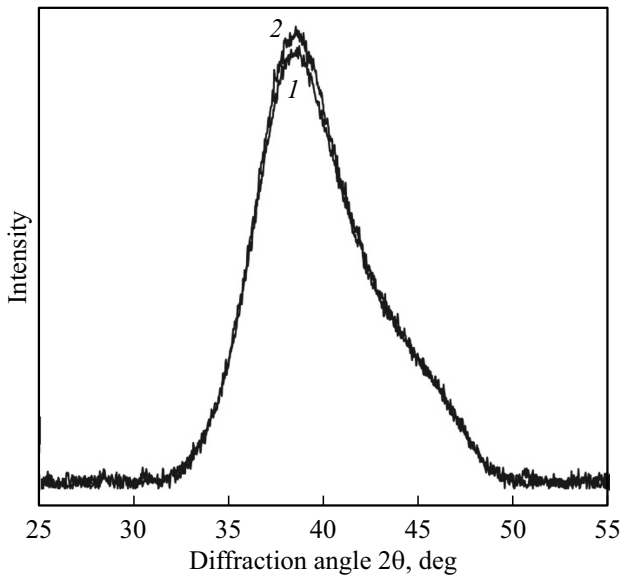


**Figure 1.** X-ray diffraction patterns of samples: curve *1* — before treatment, *2* — after treatment in an ultrasonic bath for 120 min.

Since the alloy structure consists of crystals and an amorphous matrix at the initial stage of crystallization, the overlapping peaks were divided into components corresponding to diffusion scattering from the amorphous phase and diffraction reflection from crystals. Figure 2 shows X-ray diffraction patterns of the sample before (Figure 2, *a*) and after ultrasonic treatment for 120 min (Figure 2, *b*) with the decomposition of the experimental curve into diffusion and diffraction components. Number designations in Figure 2: *1* — the experimental curve obtained, *2* — the sum of the diffusion and diffraction curves after decomposition (the sum of the curves *3, 4* and *5*), *3* and *4* — diffusion scattering from two amorphous phases, *5* — reflection (111) from aluminum crystals. The formation of two amorphous phases is often observed in amorphous alloys of the Al-TM-RE type under external impact (for example, in case of thermal or deformation treatment) or as a result of obtaining an amorphous alloy [40,41]. The different angular positions of the diffusion peaks (curves *3* and *4* in Figure 2) indicate the presence of regions with different distances between atoms, i. e., the formation of regions with different types of short-range order. According to the Ehrenfest equation, the amorphous phase described by a diffusion peak at smaller angles $2\theta$ (curve *3*) is characterized by a large radius of the first coordination sphere. The amorphous phase, described by a peak at large angles of $2\theta$ (curve *4*), is characterized by a smaller radius of the first coordination sphere (or a smaller value of the shortest distance between atoms). The difference in angular positions may be attributable to both the presence of regions with different densities and the heterogeneous distribution of components. The studied amorphous alloy includes aluminum, nickel and yttrium. The atomic radii of these elements are 1.43, 1.24, and 1.81 Å for aluminum, nickel, and yttrium, respectively. The amorphous phase with a large radius of the first coordination sphere is enriched with an element with a large atomic radius, i. e. yttrium. The amorphous phase with a smaller radius of the first coordination sphere is correspondingly depleted of yttrium. The radii of the first coordination sphere of the two amorphous phases are 2.87 Å (curve *3*) and 2.54 Å (curve *4*) in the original sample, which was not exposed to ultrasonic treatment. The change of the radius of the first coordination sphere of both amorphous phases (curves *3* and *4*) in the samples after ultrasonic treatment compared with the original sample is within the experimental accuracy.

The calculation of the integral intensity of reflection from aluminum crystals showed that the number of nanocrystals formed in the amorphous phase as a result of 120 min ultrasonic treatment is small. The average size of nanocrystals is no more than 8 nm. The average size of nanocrystals virtually did not change with an increase of the duration of ultrasonic treatment to 270 min (the change is within the error range) and was about 9 nm.

### 3.2. Treatment in ultrasonic disperser

A similar treatment of the original samples was conducted in an ultrasonic disperser. The samples were treated in a disperser for the same period of time as in an ultrasonic bath (120 and 270 min). Figure 3 shows X-ray diffraction patterns of samples treated in an ultrasonic disperser: *a*) for 120 min and *b*) for 270 min. A crystalline phase is also formed after treatment in an ultrasonic disperser: a small sharp peak appears (it is indicated by an arrow in the figure) at the top of the diffusion peak (Figure 3, *a*), which corresponds to diffraction reflection from aluminum crystals. An increase of the intensity of this peak is observed with an increase of the duration of ultrasound treatment.

As the ultrasonic treatment time increases (curve *2* in Figure 4) the additional arm on the X-ray diffraction pattern from large angles $2\theta$ becomes more pronounced (shown by arrow), which indicates a change of the structure of the amorphous phase during ultrasonic treatment.

Figure 5 shows the X-ray diffraction patterns of the samples with the decomposition of the experimental curve into components. The analysis showed that the change of the radii of the first coordination sphere of the amorphous phases in the samples treated in an ultrasonic disperser is within the limits of experimental accuracy. A pronounced arm from large angles on the X-ray diffraction pattern of a sample that has been subjected to longer treatment in an ultrasonic disperser is a sign of the appearance of heterogeneities in the amorphous phase.

Based on the calculation of the integral reflection intensity, it was found that after ultrasonic treatment in a disperser for 120 min, the proportion of nanocrystals formed is also small. The average size of nanocrystals is about 35 nm. With an increase of the treatment time to 270 min, the size of nanocrystals markedly increases (the average crystal size is about 100 nm).

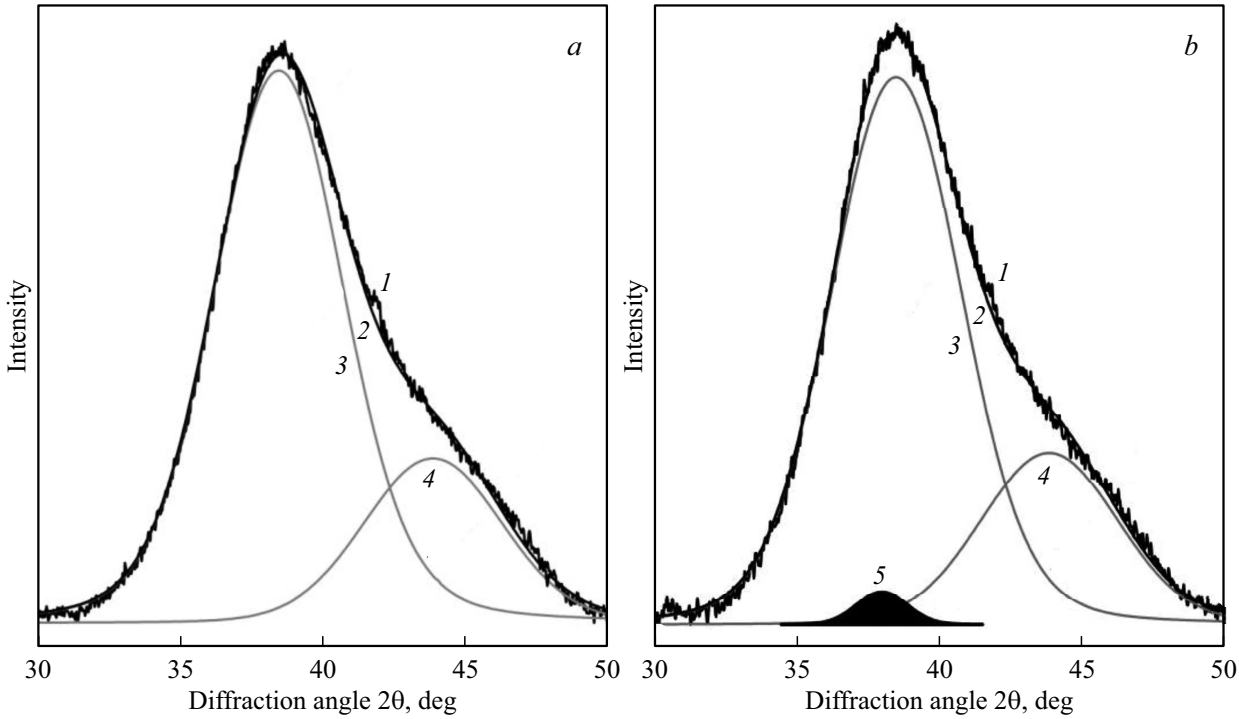


**Figure 2.** X-ray patterns of samples with separated peaks: *a*) before treatment, *b*) after treatment in an ultrasonic bath for 120 min (*1* — experimental curve, *2* — total curve, *3* and *4* — diffusion scattering from amorphous phases, *5* — diffraction reflection (111) from aluminum crystals).

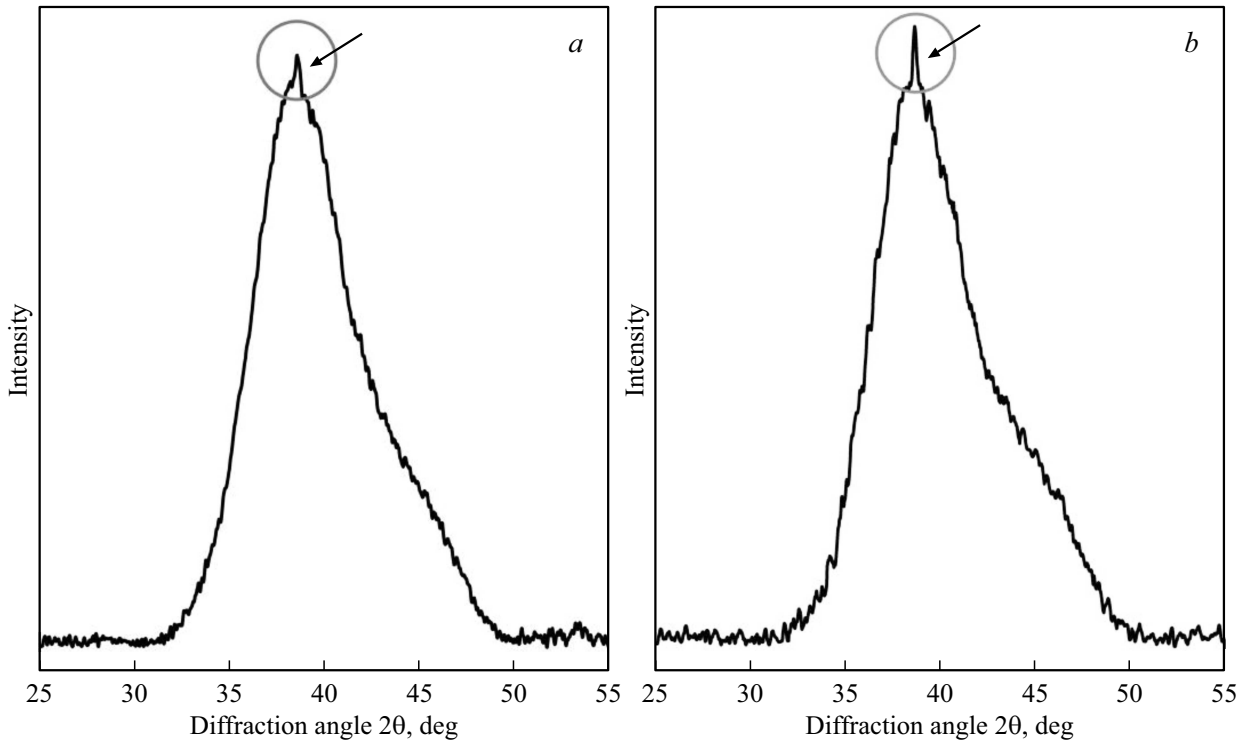


**Figure 3.** X-ray diffraction patterns of samples after treatment in an ultrasonic disperser for *a*) 120 min, *b*) 270 min.

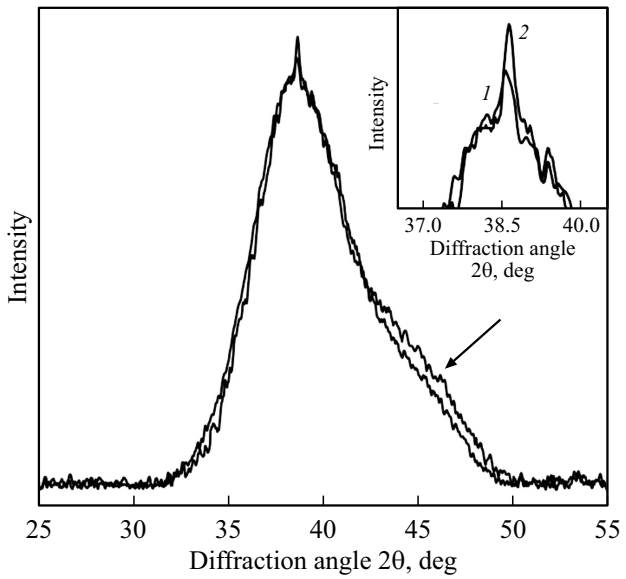


**Figure 4.** X-ray diffraction patterns of samples after treatment in an ultrasonic disperser: curve *1* — 120 min, *2* — 270 min.

The obtained results indicate that the crystallization processes begin in the amorphous phase in case of ultrasonic treatment. The number of nanocrystals is small and practically does not change with the change of ultrasonic treatment conditions. The average size of nanocrystals, on the contrary, significantly depends on the conditions of ultrasonic exposure.

The following results were obtained in the study:

• treatment in an ultrasonic bath promotes the formation of nanocrystals; the size of nanocrystals is 8 nm in case of treatment for 120 min; the size of nanocrystals practically does not change with the increase of the treatment time;

• an increase of the power of ultrasonic treatment (treatment in an ultrasonic disperser) leads to the formation of nanocrystals of a larger size, which is 35 nm in case of treatment for 120 min; the size of nanocrystals markedly increases with the increase of the treatment time.

Thus, both ultrasonic treatment (with the used parameters) and plastic deformation lead to the formation of crystals in amorphous alloys. As noted earlier, crystals are mainly formed in case of the plastic deformation in areas with a high free volume content (shear bands). The shear bands, characterized by an increased free volume content, are also characterized by a higher value of the diffusion coefficient. The diffusion constant can be 5–6 orders of magnitude higher than the undeformed part of the amorphous phase [42]. Therefore, an increase of the free volume content may be a possible reason for the appearance of crystals in the amorphous phase in case of ultrasonic treatment. The presence of free volume helps to accelerate the crystallization process; the conditions of crystal nucleation and growth can significantly change in samples with a high content of free volume. Since the

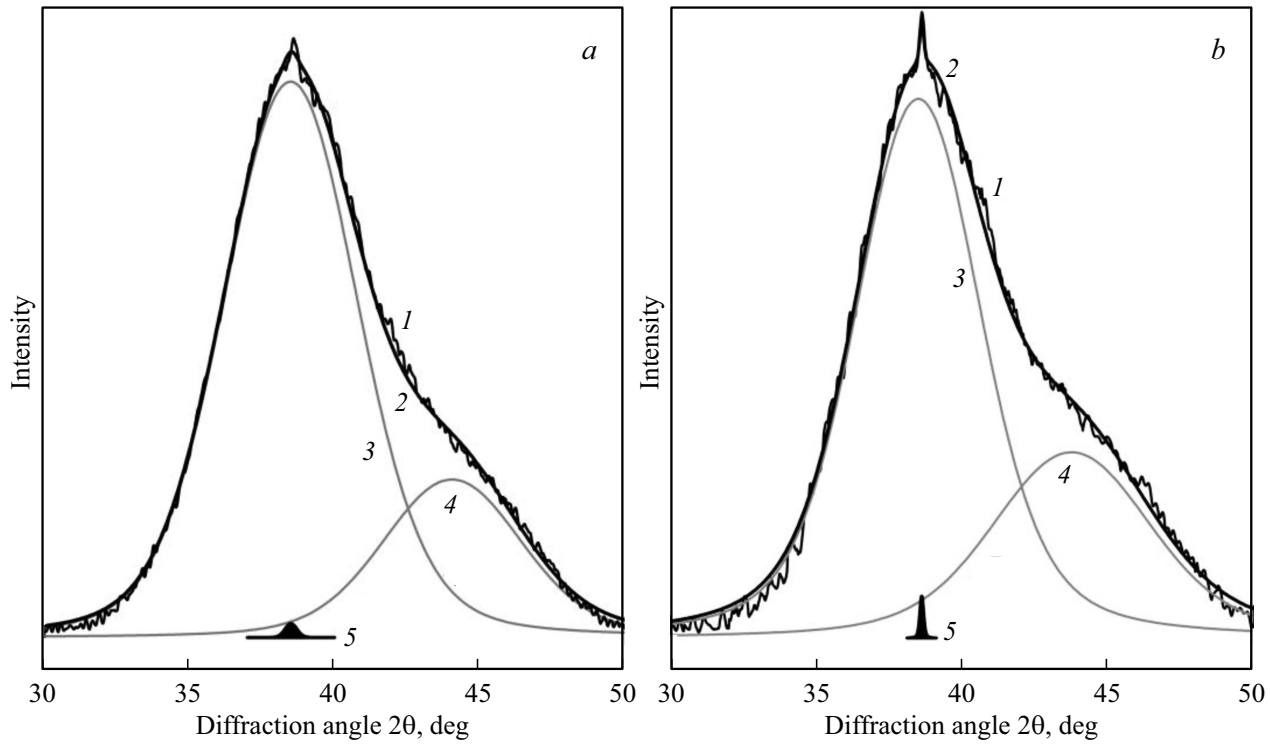


**Figure 5.** X-ray diffraction patterns of samples after treatment in an ultrasonic disperser with separated peaks: *a*) 120 min, *b*) 270 min (*1* — experimental curve, *2* — total curve, *3* and *4* — diffusion scattering from amorphous phases, *5* — diffraction reflection (111) from aluminum crystals).

proportion of crystals formed is small, and the effect of ultrasonic treatment was more pronounced in the size of the crystals formed, it can be assumed that the conditions of crystal growth significantly changed in case of ultrasonic treatment.

## 4. Conclusion

A study of the effect of ultrasonic treatment on the evolution of the structure of an amorphous alloy $Al_{87}Ni_8Y_5$ showed that ultrasonic treatment promotes the formation of a small number of aluminum nanocrystals in the amorphous phase. The reasons for the appearance of nanocrystals are discussed in the context of free volume. Changing the conditions of ultrasonic treatment (duration and power) leads to a change of the parameters of the resulting structure; physical properties of alloys can be determined by varying the free volume content in the amorphous phase. The obtained results agree well with literature data [36].

### Conflict of interest

The authors declare that they have no conflict of interest.

## References


[1] A. Inoue. Prog. Mater. Sci. **43**, *5*, 365 (1998). https://doi.org/10.1016/S0079-6425(98)00005-X

[2] B. Rusanov, V. Sidorov, P. Svec, P. Svec Sr, D. Janickovic, A. Moroz, L. Son, O. Ushakova. J. Alloys Compd. **787**, 448 (2019). https://doi.org/10.1016/j.jallcom.2019.02.058

[3] A. Sahu, R. Maurya, T. Laha. Adv. Eng. Mater. **26**, *1*, 2301150 (2024). https://doi.org/10.1002/adem.202301150

[4] A. Inoue, K. Ohtera, A.-P. Tsai, T. Masumoto. Jpn. J. Appl. Phys. **27**, *4A*, L479 (1988). https://doi.org/10.1143/JJAP.27.L479

[5] A. Inoue, T. Ochiai, Y. Horio, T. Masumoto. Mater. Sci. Eng. A **179**–**180**, *Part 1*, 649 (1994). https://doi.org/10.1016/0921-5093(94)90286-0

[6] A.L. Greer. Mater. Sci. Eng. A **304**–**306**, 68 (2001). https://doi.org/10.1016/S0921-5093(00)01449-0

[7] A.-P. Tsai, T. Kamiyama, Y. Kawamura, A. Inoue, T. Masumoto. Acta Mater. **45**, *4*, 1477 (1997). https://doi.org/10.1016/S1359-6454(96)00268-6

[8] Y.H. Kim, A. Inoue, T. Masumoto. Mater. Trans. JIM **32**, *4*, 331 (1991). https://doi.org/10.2320/matertrans1989.32.331

[9] M.C. Gao, F. Guo, S.J. Poon, G.J. Shiflet. Mater. Sci. Eng. A **485**, *1*–*2*, 532 (2008). https://doi.org/10.1016/j.msea.2007.08.009

[10] A. Anghelus, M.-N. Avettand-Fénoël, C. Cordier, R. Taillard. J. Alloys Compd. **651**, 454 (2015). https://doi.org/10.1016/j.jallcom.2015.08.102

[11] P. Rizzi, A. Habib, A. Castellero, L. Battezzati. Intermetallics **33**, 38 (2013). https://doi.org/10.1016/j.intermet.2012.09.026

[12] R.J. Hebert, J.H. Perepezko, H. Rösner, G. Wilde. Beilstein J. Nanotechnol. **7**, 1428 (2016). https://doi.org/10.3762/bjnano.7.134

[13] F.G. Cuevas, S. Lozano-Perez, R.M. Aranda, R. Astacio. Metals **10**, *4*, 443 (2020). https://doi.org/10.3390/met10040443

[14] L. Battezzati, P. Rizzi, V. Rontó. Mater. Sci. Eng. A **375**–**377**, 927 (2004). https://doi.org/10.1016/j.msea.2003.10.042

[15] Z.H. Huang, J.F. Li, Q.L. Rao, Y.H. Zhou. Mat. Sci. Eng. A **489**, *1*–*2*, 380 (2008). https://doi.org/10.1016/j.msea.2007.12.027

[16] J. Bokeloh, N. Boucharat, H. Rösner, G. Wilde. Acta Mater. **58**, *11*, 3919 (2010). https://doi.org/10.1016/j.actamat.2010.03.035

[17] N. Boucharat, R. Hebert, H. Rösner, R. Valiev, G. Wilde. Scripta Materialia **53**, *7*, 823 (2005). https://doi.org/10.1016/j.scriptamat.2005.06.004

[18] N. Boucharat, R. Hebert, H. Rósner, R.Z. Valiev, G. Wilde. J. Alloys Compd. **434**–**435**, 252 (2007). https://doi.org/10.1016/j.jallcom.2006.08.128

[19] H. Rösner, C. Kübel, S. Ostendorp, G. Wilde. Metals **12**, *1*, 111 (2022). https://doi.org/10.3390/met12010111

[20] S.V. Vasiliev, A.I. Limanovskii, V.M. Tkachenko, T.V. Tsvetkov, K.A. Svyrydova, V.V. Burkhovetskii, V.N. Sayapin, O.A. Naumchuk, A.S. Aronin, V.I. Tkatch. Mater. Sci. Eng. A **850**, 143420 (2022). https://doi.org/10.1016/j.msea.2022.143420

[21] A.L. Greer, Y.Q. Cheng, E. Ma. Mater. Sci. Eng. R Rep. **74**, *4*, 71 (2013). https://doi.org/10.1016/j.mser.2013.04.001

[22] C. Liu, V. Roddatis, P. Kenesei, R. Maaß. Acta Materialia **140**, 206 (2017). https://doi.org/10.1016/j.actamat.2017.08.032

[23] V. Astanin, D. Gunderov, V. Titov, R. Asfandiyarov. Metals **12**, *8*, 1278 (2022). https://doi.org/10.3390/met12081278

[24] P. Ramachandrarao, B. Cantor, R.W. Cahn. J. Mater. Sci. **12**, *12*, 2488 (1977). https://doi.org/10.1007/BF00553936

[25] A.R. Yavari, K. Georgarakis, J. Antonowicz, M. Stoica, N. Nishiyama, G. Vaughan, M. Chen, M. Pons. Phys. Rev. Lett. **109**, 085501 (2012). https://doi.org/10.1103/PhysRevLett.109.085501

[26] R.J. Hebert, J.H. Perepezko. Metall. Mater. Trans. A **39A**, *8*, 1804 (2008). https://doi.org/10.1007/s11661-007-9347-7

[27] G. Wilde, H. Rösner. Appl. Phys. Lett. **98**, *25*, 251904 (2011). https://doi.org/10.1063/1.3602315

[28] S. Scudino, K.B. Surreddi. J. Alloys Compd. **708**, 722 (2017). https://doi.org/10.1016/j.jallcom.2017.03.015

[29] Y. Lou, X. Liu, X. Yang, Y. Ge, D. Zhao, H. Wang, L.-C. Zhang, Z. Liu. Intermetallics **118**, 106687 (2020). https://doi.org/10.1016/j.intermet.2019.106687

[30] L. Yang, S. Xu, Y. Lou. Front. Mater. **8**, 801991 (2021). https://doi.org/10.3389/fmats.2021.801991

[31] Y. Lou, L. Yang, S. Xv, J. Ma. Intermetallics **142**, 107467 (2022). https://doi.org/10.1016/j.intermet.2022.107467

[32] M.A. Margulis. Osnovy zvukokhimii. Vysshaya shkola, M. (1984). p. 272. (in Russian).

[33] V.A. Akulichev, V.N. Alekseev, V.A. Bulanov. Periodicheskie fazovye prevrashcheniya v zhidkostyakh. Nauka, M. (1980). p. 280. (in Russian).

[34] H.N. Kim, K.S. Suslick. Crystals **8**, *7*, 280 (2018). https://doi.org/10.3390/cryst8070280

[35] W. Song, X. Meng, Y. Wu, D. Cao, H. Wang, X. Liu, X. Wang, Z. Lu. Sci. Bull. **63**, *13*, 840 (2018). https://doi.org/10.1016/j.scib.2018.04.021

[36] G. Abrosimova, V. Chirkova, D. Matveev, E. Pershina, N. Volkov, A. Aronin. Metals **13**, *6*, 1090 (2023). https://doi.org/10.3390/met13061090

[37] A.F. Skryshevsky. Strukturnyj analiz zhidkostej i amorfnykh tel. Vysshaya shkola, M. (1980). p. 328. (in Russian).
[38] A.A. Rusakov. Rentgenografiya metallov. Atomizdat, M. (1977). p. 480. (in Russian).
[39] G.E. Abrosimova, A.S. Aronin, N.N. Kholstinina. Phys. Solid State **52**, *3*, 445 (2010).
[40] G. Abrosimova, A. Aronin, A. Budchenko. Mater. Lett. **139**, 194 (2015). https://doi.org/10.1016/j.matlet.2014.10.076
[41] G.E. Abrosimova, A.S. Aronin. J. Surface Investigation: X-Ray, Synchrotron. Neutron Techniques **9**, *1*, 134 (2015).
[42] A.S. Aronin, D.V. Louzguine-Luzgin. Mech. Mater. **113**, 19 (2017). https://doi.org/10.1016/j.mechmat.2017.07.007

*Translated by A.Akhtyamov*